Title: Ru and Ni - privileged metal combination for environmental nanocatalysis

Author: Jarosław Polański, Daniel Lach, Maciej Kapkowski, Piotr Bartczak, Tomasz Siudyga, Adam Smoliński

Citation style: Polański Jarosław, Lach Daniel, Kapkowski Maciej, Bartczak Piotr, Siudyga Tomasz, Smoliński Adam. (2020). Ru and Ni - privileged metal combination for environmental nanocatalysis. "Catalysts", (2020), Vol. 10, iss. 9, art. no. 992. DOI: 10.3390/catal10090992

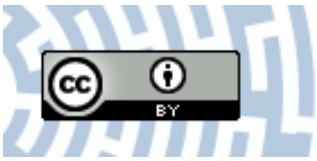

catalysts

MDPI

Review

Ru and Ni—Privileged Metal Combination for Environmental Nanocatalysis

Jaroslaw Polanski [1,*], Daniel Lach [1], Maciej Kapkowski [1], Piotr Bartczak [1], Tomasz Siudyga [1] and Adam Smolinski [2]

[1] Faculty of Science and Technology, Institute of Chemistry, University of Silesia, Szkolna 9, 40-006 Katowice, Poland; daniel.lach@us.edu.pl (D.L.); maciej.kapkowski@us.edu.pl (M.K.); piotr.bartczak@us.edu.pl (P.B.); tomasz.siudyga@us.edu.pl (T.S.)

[2] Central Mining Institute, Plac Gwarkow 1, 40-166 Katowice, Poland; smolin@gig.katowice.pl

* Correspondence: polanski@us.edu.pl; Tel.: +48-32-259-99-78

Received: 3 August 2020; Accepted: 18 August 2020; Published: 1 September 2020

Abstract: Privileged structures is a term that is used in drug design to indicate a fragment that is popular in the population of drugs or drug candidates that are in the application or investigation phases, respectively. Privileged structures are popular motifs because they generate efficient drugs. Similarly, some elements appear to be more efficient and more popular in catalyst design and development. To indicate this fact, we use here a term privileged metal combination. In particular, Ru-based catalysts have paved a bumpy road in a variety of commercial applications from ammonia synthesis to carbon (di)oxide methanation. Here, we review Ru/Ni combinations in order to specifically find applications in environmental nanocatalysis and more specifically in carbon (di)oxide methanation. Synergy, ensemble and the ligand effect are theoretical foundations that are used to explain the advantages of multicomponent catalysis. The economic effect is another important issue in blending metal combinations. Low temperature and photocatalytic processes can be indicated as new tendencies in carbon (di)oxide methanation. However, due to economics, future industrial developments of this reaction are still questionable.

Keywords: Ru/Ni combinations; synergy; ensemble effect; ligand effect; environmental nanocatalysis; low temperature carbon (di)oxide methanation; ultra-low temperature carbon oxide methanation

1. Introduction

With the ever increasing human population, responsibly interacting with the environment is becoming more and more important. Although it is still not certain whether the anthropogenic contribution is the cause of the climate changes that are occurring, there are good arguments that support this point of view [1–3]. Our carbon footprint is an inevitable sign of human life and civilization, and the paradox is that excess carbon could endanger our continued existence. In other words, environmental sustainability should guide our current rules for managing the environment. Recently, there have been a variety of chemical concepts that have been proposed to address these problems, in particular, the green chemistry principle [4], which stresses the importance of the energy and material efficiency that is associated with minimal risk and safe chemistry. Catalysis is at the center of this concept because by definition it enables chemical processes to be enhanced by using only a small number of catalysts, i.e., substances that might increase the reaction rates. Accordingly, by using a sub-stoichiometric quantity of a catalyst, we can manipulate the stoichiometric quantities of the reaction products. This means that catalysis is an energy- and material-efficient method. Rodriguez-Padron et al. [5] estimated that currently as much as ca. 90% of the processes that are used in food, health, fuel and energy–related chemicals involve at least one catalytic step. The environmental catalysis concept involves issues such

as the "catalytic decomposition of pollutants for air, water and soil remediation, hydrogen production, CO_2 reduction and biomass valorization" [5].

Environmental catalysis is of key importance for contemporary civilization. For example, a solution for mitigating ecotoxic carbon dioxide overproduction could significantly help to develop more sustainable chemistry. To illustrate the potential of this issue, let us imagine a future that is based on the renewable fuels that are produced from CO_2 in the refineries that are operated using economically and environmentally friendly chemistry. This would make CO_2 an asset rather than a waste [6].

The activity of catalysts critically depends upon its structure. Accordingly, the combination of metals within a nanocatalyst provides an opportunity to extensively manipulate the structure, which is a chance to discover unexpected reactivity and to investigate the structure–reactivity relationships. This would enrich our knowledge about the design protocols of potentially active nanocatalyst systems and would also produce novel active catalyst candidates. Bimetallic particles are an important form of metal combination, which gained in importance with the inception of the Sinfelt concept of bimetallic clusters [7,8]. Historically, the term bimetallic catalysis was coined by Exxon in 1960. Bimetallics can be further organized as the crown-jewel, hollow, hetero, core-shell or alloyed structures. An example can be supported bimetallic gold and palladium nanoparticles. An introduction to their synthesis, structure and application in environmental catalysis can be found in [7]. Here we would like to illustrate how popular some metal combinations in catalysis are, not only as formally bimetallic structures, but in a more general sense of a multi-component systems. Recently, an increasing amount of interest has been devoted to using such systems in environmental engineering. This especially includes carbon (di)oxide methanation (compare Sections 5 and 6) or biomass conversion [9–11]. A variety of metal combinations and structural forms have been reported in this area. In this review, we will focus on the Ru/Ni system, which has shown a specifically intense application in nanocatalysis.

Drug design motifs, which are especially popular in the population of drug molecules, are labeled as privileged structures. Accordingly, Ru and Ni can be seen as privileged elements in catalysis. In particular, Ru-based catalysts have paved a bumpy road in a variety of commercial applications from ammonia synthesis to carbon (di)oxide methanation. Ru/Ni combinations play a role in environmental engineering and supporting energy storage from renewable sources (photovoltaic panels, tidal power plants, wind turbines). The Ru/Ni activity in CO_2 methanaton allows energy to be stored in a form of methane (high energy product), which is used as a fuel for generating power in gas turbines. The stored energy can be used not only to power the existing gas networks, but could be converted into electricity, e.g., in steam and gas systems or could be pyrolyzed to H_2 needed for hydrogen fuel cells. The Ru/Ni bimetallic combination provides a variety of unique functional properties as the extension of the operation time and the limitation of carbon deposit on the catalyst surface.

2. Theoretical Ground of Multicomponent Catalysis: Synergy, Ensemble and Ligand Effects

Metal combinations are an attractive way to design novel materials for catalytic applications. One can understand the reason for this is to simply broaden the library of catalyst candidates. Bimetallics is the simplest form of these multicomponent systems, and trimetallics are a clear extension of this concept, e.g., [12]. A variety of uses of bimetallics in nanocatalysis can be found in [13].

Synergy is a term that was originally coined to describe an enhancement of the activity of a drug if instead of a single medicine we use a combination of drugs. The pragmatic rule of "working together is better than working alone" goes well beyond the search for synergy. For years, synergy was too complex to be precisely controlled or designed [14]. The synergic interactions between metals enables the properties of the original single–metal system to be significantly modified and/or improved in multicomponent systems. Synergy can involve complex effects and it seems to be helpful to analyze the meaning of this concept in catalysis.

In catalysis, synergy can be described much more precisely than in medicinal chemistry. Accordingly, the terms ensemble and ligand effect have been developed to describe the molecular basis of the interactions between the elements in a catalyst system blended (Figure 1). The most obvious

forms of bimetallics are alloys. By alloying, the arrangement of the individual metals is modified. The result is referred to as the ensemble effect. This generates for example the dilution of one of the elements of a bimetallic system by a second element at the surface. An example is the dilution of surface Pd by Au. With increasing surface Au coverage, the contiguous Pd ensembles disappear and isolated Pd ensembles form. This effect explains the enhancement of the reaction rate via the formation of highly active surface sites, e.g., isolated Pd pairs. In turn, the ligand effect describes the interactions between the elements of a catalyst, e.g., the electronic perturbation of Pd by Au [15]. For a more detailed discussion of the ensemble and ligand effects in bimetallics, the reader should see [16], and for an extensive introduction to the synergistic effect in heterogenous nanocomposite catalysis, see [17].

From the theoretical point of view, a variety of effects can be observed when metals are combined. Basically, these depend on metal properties. In Table 1, we list metal properties that can be important when designing or blending catalysts especially methanation catalysts.

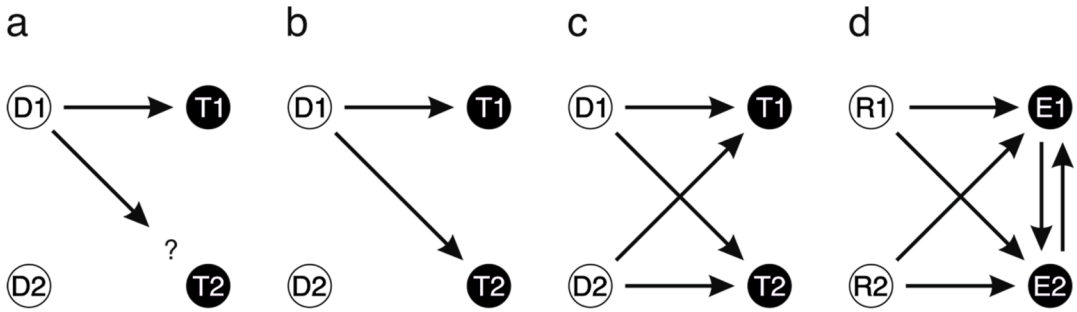

Figure 1. A comparison of the synergy term that is used in pharmacology and catalysis. Synergy allows classical drug design to be improved (**a**) by designing multi-component drugs (D1, D2) that can interact with the multitarget (T1, T2) system in the polypharmacology model (**b**) or synergy model (**c**). However, in catalysis (**d**), synergy usually involves enhancing the reactivity in a multi-reactant (R1, R2) system. In a multi-component catalyst (E1; E2), E1 and E2 can interact via the ensemble effect and the ligand effect. According to [14].

Table 1. Physicochemical properties of selected metals.

Metal [a]	Covalent Radius [b] [Å]	Surface Energies [c] [J m^{-2}]	Dissociation Energy [kJ mol^{-1}]	Ionization Energy [kJ/mol]	Electronegativity Pauling/Allen Scale	Ref.
$_{47}$Ag	1.45	1.246, 1.250	159.20 ± 2.89	I = 731.0 II = 2070 III = 3361	1.93/1.87	[18–22]
$_{46}$Pd	1.39	2.003, 2.050	<136.04	I = 804.4 II = 1870 III = 3177	2.20/1.58	[19–23]
$_{42}$Mo	1.54	2.907, 3.000	431,68 ± 0.96	I = 684.3 II = 1560 III = 2618	2.16/1.47	[19–22,24]
$_{77}$Ir	1.41	3.048, 3.000	357 ± 67,54	I = 880 II = 1600	2.20/1.68	[18–22]
$_{78}$Pt	1.36	2.489, 2.475	302.96 ± 1.93	I = 870 II = 1791	2.28/1.72	[19–22,25,26]
$_{76}$Os	1.44	3.439, 3.450	414.89 ± 77.19	I = 840 II = 1600	2.2/1.65	[18,20–22,26,27]
$_{27}$Co	1.26	2.522, 2.550	≤127	I = 760.4 II = 1648 III = 3232	1.88/1.84	[19–22,28]
$_{26}$Fe	1.32	2.417, 2.475	110.96 ± 8.68	I = 762.5 II =78 1561.9 III = 2957	1.83/1.80	[19–22,29]
$_{28}$Ni	1.24	2.380, 2.450	197.02 ± 0.19	I = 737.1 II = 1753.0 III = 3395	1.91/1.88	[19–22,30]

Table 1. *Cont.*

Metal [a]	Covalent Radius [b] [Å]	Surface Energies [c] [J m^{-2}]	Dissociation Energy [kJ mol^{-1}]	Ionization Energy [kJ/mol]	Electronegativity Pauling/Allen Scale	Ref.
$_{45}$Rh	1.42	2.659, 2.700	232.13 ± 0.05	I = 719.7 II = 1740 III = 2997	2.28/1.56	[19–22,31]
$_{44}$Ru	1.46	3.043, 3.050	192.97 ± 19.3	I = 710.2 II = 1620 III = 2747	2.2/1.54	[19–22,32,33]

[a] Activity in CO_2 methanation increases from Ag to Ru according to [34]. [b] Covalent radius for the specified metals based on data from [35]. [c] Surface energies (experimental data) according to [36,37], respectively.

A variety of metal combination-related effects for noble metal-based nanoparticles were reviewed in [38].

3. Environmental Catalysis Is Where Economy Drives Chemistry

Notably, early catalysis was connected with Sabatier, who investigated hydrogenation, in particular, by discovering catalytic carbon dioxide hydrogenation [39]. Originally, this goal was not a matter of environmental sustainability, but it was rather technological need and economy that inspired him. First of all, this investigation pioneered modern catalysis. With the increasing number of people inhabiting the limited area of the earth, the environmental issues have gained in importance. We are aware today that the economic aspects are directly connected with environmental issues, which is often a limiting factor in contemporary chemical technology. The environmental sustainability more and more becomes an economic issue.

It is not a coincidence because the economy controls all aspects of human activity The importance of the economic element in contemporary chemistry can be illustrated, for example, by the clear lexical association of atoms and the economy. The *atom economy* is one of the rules of green chemistry. Although the actual meaning of the *atom economy* is idiomatic and applies more to chemistry than to the economy, the clear economy-based descriptors were inspired by this approach and were analyzed in the economic dimension, e.g., the E factor—or related E + factor—the proportion of the waste material to desired products [40]. The concept of circular chemistry that is integrated with a circular economy has recently been proposed. In this concept, the sustainability of the chemical products is completed by optimizing the resource efficiency by replacing the "take-make-dispose" technologies with circular processes. Theoretically, this can provide us with a fully waste-free chemistry [41]. Sabatier's dehydrogenation research might point the way to economy-driven chemistry of carbon dioxide. He investigated the activity of the freshly reduced Ni towards various gases at temperatures between 150 and 200 °C. The inspiration was the discovery that nickel carbonyl could be formed by the action of carbon monoxide on powdered nickel [42]. Between other reactants, carbon oxide and dioxide (carbon (di)oxides) could be converted into methane in this reaction. Sabatier was aware of the catalytic action of the metal by "a real chemical combination of the surface of the metal with the surrounding gas." In his Nobel prize lecture, he indicated the poisonous effect of any contaminations. For example, the traces of thiophene blocked the hydrogenation of benzene into cyclohexane, if catalyzed by Ni. Accordingly, metal catalysis resembles the action of "ferments", i.e., the enzymes in living organisms [39].

In the language of today chemistry, in this study, a library of potential hydrogenation catalysts, was screened. As a result, copper, cobalt, iron and platinum, which can fix free hydrogen or even "take hydrogen from substances" (dehydrogenation), were discovered.

In the Sabatier model, the catalytic process on metal involves: the adsorption of the reactant on the catalyst surface, a chemical reaction and the desorption of the products. The efficient conversion of reactants into products must be a kind of homeostasis between the potential of a catalyst for the adsorption of a reactant as well as the potential for the desorption of the products resulted. Otherwise, the adsorbed reactant or product would block the surface and the reaction process could not proceed. If we analyze the catalyst's performance as a function of its adsorption energy, the activity of the metals

can be aligned to a so-called volcano plot. This problem will not be discussed further, and the reader should compare the many available references for a representative description of this effect, e.g., [43].

A variety of metals have been tested as catalyst candidates for CO_2 methanation and many of these from group VIIIB appeared to be efficient. The activity varied depending on investigations, e.g., Fisher et al. indicated the following order of decreasing activity: [44]

$$Ru > Ir > Rh > Ni > Co > Os > Pt > Fe > Mo > Pd > Ag,$$

while Graf et al. determined this as: [45]

$$Ru > Fe > Ni > Co > Rh > Pd > Pt > Ir.$$

For a number of examples of other data of this type, the reader should compare the references [46].

The differences between individual investigations are obvious. This results from the fact that metal identification alone is not the only feature that determines the activity of a catalyst. In his excellent tutorial review on understanding catalysis, Roduner uses the example of gold, which as a bulk noble metal is an unreactive and, therefore, non-catalytic material. However, as nanogold, its electronic structure resembles more that of a single gold atom and therefore the catalytic potential of the gold nanoparticles is attractive. Accordingly, the size of the nanoparticles could be a parameter that controls the catalytic performance of a material [46].

4. Ru and Ni—Privileged Elements for Catalysis

4.1. Ru and Ni for Catalysis

In the context of the applicability of ruthenium Ru in catalysis, its associations not only with Ni but also with iron Fe and platinum Pt are worth of mentioning. Both Fe and Pt have numerous applications in catalysis. In nature, Ru coexists with platinum and is obtained usually from the platinum ore. Ru is a transition metal in group VIII of the periodic table. It is a polyvalent element coexisting in the same family as iron. The configuration of Ru $4d^7 5s^1$ compares to iron Fe $3d^6 4s^2$. Accordingly, a number of d electrons are higher in Ru than in Fe. In turn, shielding effect of the inner non-d electrons is higher for Ru than Fe due to the larger distance from the nucleus of the 4d than 3d shell. Chemical valences of Ru range from +1 to +8. Ru forms tetroxide (RuO_4) and dioxide (RuO_2). In the context of environmental catalysis, the formation of a series of Ru carbonyls is worth mentioning. For further details of catalysis-related Ru or its compounds and their properties, refer to [33]. The formation of non-stoichiometric compounds by Ru compounds is worth mentioning in the context of catalysis [47].

In turn, nickel was portrayed by Sabatier as the "Spirited Horse" of Transition Metal Catalysis [48]. It is "delicate, difficult to control, and incapable of sustainable work." [49]. Like spirited horses, Ni catalysts are of great value. Ni appeared to be an efficient system that could be used in the conversions of π-electronic systems. Moreover, a variety of nanotechnologies have been described for the conjugation of Ni with carbon-based systems, in particular, nanotubes or graphene. A variety of the technical advantages of Ni-based catalysts and the substantial catalysis-related properties of Ni can be found in [48].

One of the advantages of Ni catalysis is the price of the catalysts. The prices in USD per 1 mmol of the substance compares as $NiCl_2$ 0.1 < $PdCl_2$ 5.8 < $PtCl_2$ 32.2 < $AuCl_3$ 35.6 < $RhCl_3$ 51.8. [49]. With the increasing capabilities of computations, the design of catalysts has gained in importance. Nørskov et al. drew our attention to the economic issues in catalyst design [50]. In Figure 2, we present a comprehensive analysis of the problem of combining in catalytic CO_2 methanation Fe and Ni, this time. We can observe that there is an optimum that permits the Fe/Ni activity and its economic price to be optimized [51]. Accordingly, beyond the physical interactions that occur when combining metals, which result in an ensemble and the ligand effect, we can also see the economic effect. Additionally,

because catalysis should work in industry, the economic effect of metal combination is at least equally important as the action of ensemble or ligand effects.

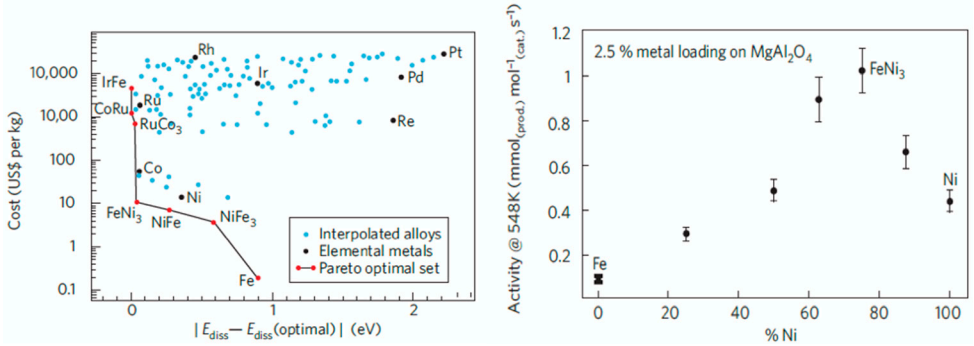

Figure 2. Designing a methanation catalyst. The price vs. the catalytic performance of a single and multicomponent (on the left) bimetallic Fe/Ni combination enables the activity of pure individual element catalysts to be increased (on the right). The catalyst can be optimized by overlapping the price (**left**) and physical synergy (**right**). © Adopted from [50,51].

More sophisticated simulations were used recently to model the Ru catalytic systems. For example, the outstanding performance of supported sub-nanometer ruthenium particles in the catalytic CO methanation inspired theoretical investigations using gas-phase ruthenium clusters where Ru_n^+ (n = 2–6) are employed as model systems to explain the reactivity of the system [52].

4.2. Physics of Metal Alloying, Combining of Ru and Ni

Combining metals can result in alloys that are either homogeneous or heterogeneous (consisting of two or more phases). Unlike homogeneous alloys, which are formed of a uniform single phase, heterogeneous alloys or unalloyed metals are multi-phase systems. Although a majority of catalytic applications refer to homogeneous single-phase systems (compare Section 2 for the discussion of the interactions between the elements in such systems), heterogeneous alloys or unalloyed systems can also be useful catalysts, e.g., [53,54].

The interphase between metals (metal oxides) affects the material properties. Essential physical effects are generated in this location. Therefore, bimetallic combinations are important for substantial technologies as batteries, bimetals, preventing corrosion, or generating electricity. Specifically, ruthenium forms alloys with the platinum group metals Ni, Pd, Pt and Co, W. Ru is widely used in technology especially in the chemical industry (catalysts in the synthesis of long-chain hydrocarbons or oxidation), automotive industry (car catalysts) and electrical engineering (Ru increases the hardness of the platinum alloys that are used to create electrical contacts and to produce resistance wires) [55]. In non-platinum group bi- or multimetal alloys, a small amount of Ru is advantageous because it often improves the quality of a material. For example, corrosion resistance in titanium alloys was increased by introducing 0.1% Ru [56]. Ru/Ni bimetallic combinations are superalloys that are widely used in jet engine turbines [57]. Several combinations that were based on Ni doped with Ru EPM-102 (3% Ru), TMS-162 (6% Ru), TMS-138 (6% Ru) or TMS-174 (6% Ru) have also been described [58–60].

Liu et al. designed a bifunctional multicomponent system (NiIrRuAl NPNWs) that was used to form nanowires that were useful for the electrochemical evolution of H_2 and O_2. This, in the form of nanoporous nanowires, which were used as a catalyst in the presence of 0.1 M $HClO_4$ at a cell voltage of 1.464 V, enabled a complete water splitting [61]. The catalytic activity was enhanced by optimizing three aspects: (I) the formation of an electrocatalyst alloy with a transition metal [8], (II) a synergistic active Ru interaction with a stable Ir and (III) the presence of a hierarchical nanostructure and uniform dispersion of the porous nanostructure [61].

Nickel-metal hydride (Ni-MH) batteries are well known as reversible energy storage systems whose energy densities (360 MJ/m^3) and capacity are among the highest that have been reported [62,63].

Their main disadvantages are that they discharge faster and have a shorter service life than NiCd-based systems. In Ni-MH, the cathode is a nickel plate and the anode is an alloy. The alloyed metals are these capable to form metal hydride with hydrogen released during charging. NiMH batteries are widely used in hybrid cars [62]. Willey et al. upgraded multicomponent alloys for the Ni-based cells by coating the surface with various metals or metal oxides from the platinum group (Ru, Pt). The advantage of such a structure was the productive hydrogen charge/discharge profile and the exceptional resistance to deactivation in air [64,65].

Shi distinguished four main synergistic catalytic effects in nanocomposite materials [17]: (I) Mutual coactivation of one component through the other component with the overall effect of enhancing the catalytic properties of the nanocomposite; (II) in multistage reactions, the successive catalytic interaction of two components to increase the activity or selectivity of the reaction; (III) in long term catalytic reactions, the protective effect of one component over another by the degradation of the main component. (IV) In complex redox reactions, the storage or the release of reagents by catalytic assistance. The above-mentioned effects can overlap and a resulted complex network of additive or inhibitory effects can affect the catalytic activity of nanosystems. Defects in the crystal lattice and the presence of a bimetallic alloy in the vicinity of the nanosystem also play a role in catalytic activity of the nanomaterial. Chen et al. showed that monometallic sites with higher activity are optimal locations for a formation of bimetallic sites [66]. The downsizing effects on nanoparticles below the critical value of 2.7 nm can involve changes of the adsorption force or oxidation state, and changes of the electronic structure by a formation of two-metal alloys. The length of metal-metal bonds can be modified and eventually geometric effects can be manipulated by a formation of heteroatom bonding. This results in new electronic structures at the interface of bimetallic nanocomposites [67].

Actually, the multicomponent structures not only involve metals alone but also metal combinations in compounds (i.e., the chemical compounds of the individual components), in particular, metal oxides. The Schottky effect is an example of the physical effects that originate at the contact between neighboring elements and could crucially influence catalytic activity of the systems (Figure 3).

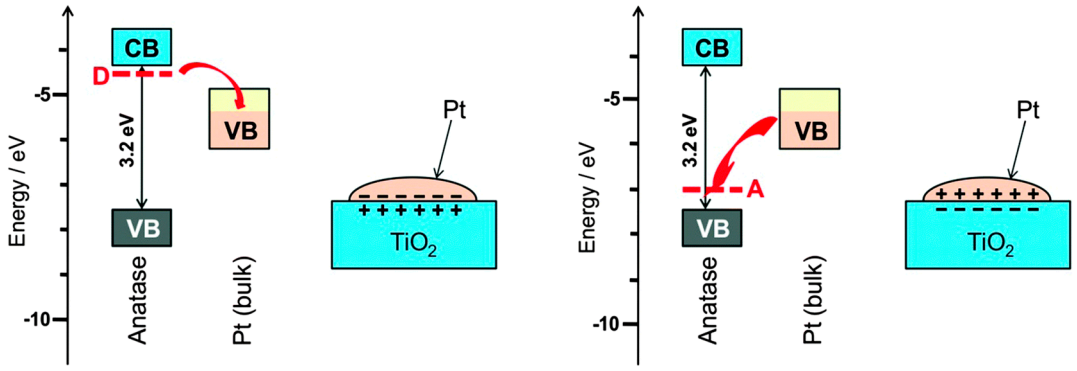

Figure 3. Schottky contacts in a Pt/TiO_2 (anastase), which can strongly affect the catalytic properties of a system (**right**). Additional charge-compensating electrons at the neighboring Ti atoms can occur as a result of the presence of an HO impurity in TiO_2 (**left**). Its location is below the conduction band (CB). The transfer of the donor state electrons to the partially filled valence band (VB) of the metal (Pt) creates a charge-polarized interface. © Adopted from [43,68].

Metal combination is an important manipulation in a variety of nanotechnologies. Electrochemical condensers (EC) are an illustrative example. EC can be grouped into three main classes: pseudocapacitors (redox supercapacitors), electrochemical double layer capacitors (EDLC) and hybrid capacitors [67] whose functional properties are limited by parameters such as density and maximum power output. Morag et al. described a symmetric pseudocapacitive supercapacitor that was constructed of Ru/RuO_2 applied on Ni foil with a polystyrene distance. This combination appeared to be especially successful and had fast scan rates, a high-power density and an excellent capacitance retention [69]. The advantageous pseudocapacitive properties of RuO_2 resulted from its specific

capacitance, high conductivity and stable cycling performances [70]. Similar to TiO and IrO_2, RuO_2 has low resistivity, which is advantageous for the absorption on the electrodes surface of non–typical metallic materials [71].

A variety of examples of the use of Ru/Ni systems can be found in environmental engineering. Jeong et al. described direct methanol fuel cells (DMFCs) that were active at 300–400 °C with the Ru/Ni catalyst, whereas the Ru nanoparticles were sitting on the porous Ni mesh [57]. The ALD (atomic layer deposition) method, which is used to construct the Ni/ALDRu system, appeared to be advantageous for electrochemical oxidation of methanol because the above mentioned catalysts do not suffer from poisoning in the presence of the CO leftovers [58,59]. In practice, Pt and Ru bimetallics are currently being used for this purpose. The electronic interactions between these elements play a role in high oxidation performance [57,60,61]. In turn, the Ru/Ni catalyst system in a DMFC (direct methanol fuel cell) yields a highly efficient hydrocarbon oxidation and reforming below 500 °C limiting the tendency for coal deposition [57,62,72]. Modafferi et al. constructed an intermediate temperature solid oxide fuel cell (IT–SOFCs) in the auto–thermal reforming (ATR) process. When used for the steam reforming (SR) of propane, the Ni–Ru/GDC catalyst (GDC—porous gadolinia–doped ceria electrode) had the highest performance at 700 °C [63]. Similar systems have been investigated by Uchida et al. in SOFCs (solid oxide fuel cell) that were fed with methane at 800 °C. In this particular case, up to 3% nanometric Ru was dispersed in order to improve the anode efficiency. Although the coal deposition in the ATR (auto-thermal reforming) process was confined in the SR process (steam reforming), the catalyst was deactivated. The presence of oxygen increased the CO_2 and H_2O fractions but the Ni–Ru/GDC (GDC—porous gadolinia–doped ceria electrode) catalyst remained highly active despite the observed degasification of the coal deposits [64,65]. It has been found that Ru in the Ni–Ru/GDC system in SOFC fed with C_1–C_4 gases promoted reforming. At the same time, coal deposition on anode was decreased [17]. Similar systems were investigated by Lee at al., who constructed a thin film single-chamber SOFC with a nano–dendric anode Ru–GDC (GDC—porous gadolinia–doped ceria electrode). In fuel production, these systems had better catalytic activity and thermal stability than the analogous Ni–GDC systems [66]. The cathode was constructed from perovskites using a sputter or pulsed laser deposition (SSC or LSCF, respectively). In addition, the surface of the material was covered with an Au nanocoating in order to improve its electrical conductivity [66].

4.3. Ru and Ni Combinations—Preparation and Applications

Alshammari et al. recently reviewed Au/Pd bimetallics in environmental nanocatalysis, which can be synthesized by: impregnation, deposition–precipitation, chemical and physical vapor deposition, co–precipitation or liquid preparation [7]. In Table 2, we have compiled the examples of preparation and application of Ru/Ni systems.

Table 2. Preparation and application of Ru/Ni systems.

Composition	Preparation Method	Application	Ref.
Ti-0.1 wt.% Ru, Ti-3 wt.% Al-2.5 wt.% V-0.1 wt.% Ru, Ti-6 wt.% Al-4 wt.% V-0.1 wt.% Ru	melting	increasing the corrosion resistance of titanium alloys	[56]
Ni-24 wt.% Al-2 wt.% Ru, Ni-9.4 wt.% Al-5.7 wt.% Ru	melting	superalloys	[57]
Ni-34.1 wt.% other metals-2 wt.% Ru	melting	superalloys	[58]
Superalloy with 2–3 wt.% Ru	melting	improved the microstructural stability of superalloys	[59]
Ni alloys with 2–9 wt.% Ru	melting	superalloys	[60]
Ni/Ru/RuO_2	Ru deposition/Ni etching cycles, electrochemical oxidation	supercapacitor electrode	[69]
NiAlIrRu nanoporous nanowires-variable composition	melting and dealloying	electrocatalytic O/H evolution reaction (OER/HER)	[61]
Ru coated MnAlCoMnNi alloy	reduction of Ru complex	improvement of the hydrogenation properties of nickel-metal hydride battery alloy	[62,64]
3.3 at% Pd–0.6 at% Ru coated commercial nickel metal hydride electrode alloy	hydrazine reduction of metal precursors	enhanced the kinetics at low temperatures—nickel-metal hydride battery alloy	[65]

Table 2. *Cont.*

Composition	Preparation Method	Application	Ref.
1.5% Ru/Ni	selective etching with nanoparticle transfer	methanation	[53]
1.44 wt.% Ru/Ni	selective etching with nanoparticle transfer	methanation	[73]
3% Ru–30% Ni/$Ce_{0,9}Zr_{0,1}O_2$	one pot hydrolysis of metal nitrates, calcination	methanation	[74]
1.0% Ru/Ni nanowires	Ni precursor wet reduction, selective etching with nanoparticle transfer	methanation	[75]
0.5% Ru–20%Ni/Al_2O_3	wet impregnation, calcination	methanation	[76]
1% Ru–15% Ni/CeO_2-ZrO_2	sequential wet impregnation, calcination	methanation/reverse water–gas shift	[77]
Ni-Ru/ZrO_2	wetness impregnation, calcination	methanation	[78]
0.39 wt.% Ru/NiMgAl	co-precipitation, wet impregnation, calcination	CO_2 methanation	[79]
9.2 wt.% Ni–0.8 wt.% Ru/SiO_2	impregnation, calcination	CO methanation	[80]
6.5 wt.% Ni@Ru-La_2O_3/SiO_2	wetness impregnation, calcination	CO methanation	[81]
20 wt.% Ni–0.5 wt.% Ru/SiO_2	wetness impregnation, calcination	CO methanation	[82]
5 wt.% Ni–1 wt.% Ru/Al_2O_3, 5 wt.% Ni–1 wt.% Ru/YSZ, 5 wt.% Ni–1 wt.% Ru/$MgAl_2O_4$	wet impregnation, calcination	dry reforming of methane	[83]
15 wt.% Ni–0.5 wt.% Ru/MgO/Al_2O_3	wet impregnation, calcination	dry reforming of methane	[84]
14 wt.% Ni–1 wt.% Ru/CeO_2-Al_2O_3	co-precipitation, wet impregnation, calcination	hydrogen production via steam reforming of simulated bio-oil	[10]
10 wt.% Ni–1 wt.% Ru/C	incipient-wetness impregnation, calcination	hydrogenolysis of lignin	[11]
Ni-Ru (various loading)/C	chemical reduction, galvanic replacement, calcination	catalic hydrogenation	[85,86]
1 wt.% Ni–0.3 wt.% Ru/ZnSe: CGSe	flux-assisted method, precipitation	photocatalytic hydrogen evolution	[87]

5. Carbon (Di)oxide Methanation

Carbon dioxide can be seen as a prospective raw material that enables the synthesis of a number of carbonous products as well as being the basis for developing novel energy and fuel engineering technologies. Carbon di(oxide) methanation is one of the potential solutions for atmospheric carbon recirculation. CO_2 methanation is often expressed by the following simple equation [88]:

$$CO_2 + 4H_2 \rightarrow CH_4 + 2H_2O \quad \Delta H = -165 \text{ kJ/mol}$$

Actually, this process involves a complex collection of reactions [89]. CO_2 methanation is thermodynamically favorable. However, economics, which is determined by energy issues, is an important limitation of the current technologies [46,73,90,91]. Kinetics requires that catalysts be used in methanation. Figure 4 illustrates that the thermodynamics K constants define a low temperature as the most advantageous area for the process. The methanation of CO, solar CO or syngas (mixtures of CO and H_2) are related issues in environmental chemistry [7,73,92].

Reaction no.	Reaction formula	$\Delta H_{298\,K}$ (kJ mol^{-1})	$\Delta G_{298\,K}$ (kJ mol^{-1})
R1	$CO + 3H_2 \leftrightarrow CH_4 + H_2O$	−206.1	−141.8
R2	$CO_2 + 4H_2 \leftrightarrow CH_4 + 2H_2O$	−165.0	−113.2
R3	$2CO + 2H_2 \leftrightarrow CH_4 + CO_2$	−247.3	−170.4
R4	$2CO \leftrightarrow C + CO_2$	−172.4	−119.7
R5	$CO + H_2O \leftrightarrow CO_2 + H_2$	−41.2	−28.6
R6	$2H_2 + C \leftrightarrow CH_4$	−74.8	−50.7
R7	$CO + H_2 \leftrightarrow C + H_2O$	−131.3	−91.1
R8	$CO_2 + 2H_2 \leftrightarrow C + 2H_2O$	−90.1	−62.5

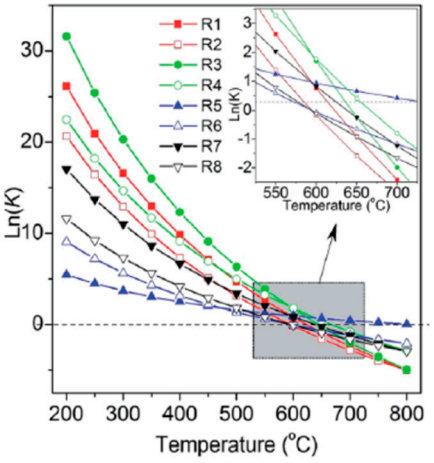

Figure 4. The reactions that are involved in CO_2 methanation and their calculated thermodynamic equilibrium constants. A significant decrease of K vs. temperature can be observed. © Adopted from [89,93].

6. Ru/Ni Catalysts for Low-Temperature CO_2 (CO) Methanation

Ni-based systems are often a good compromise between a high catalytic activity and a low price, which is important in the current chemical industry often based on heterogeneous catalysis [94–96]. However, nickel catalysts have a poor activity at low temperatures. They can also easily get deactivated at high temperatures by sintering and/or coke deposition and are particularly susceptible to sulfur poisoning, e.g., from H_2S [80,91,97]. There are several solutions that can improve the performance and life span of this type of catalyst, for instance, using a support [83,91,98–100], catalytic promoters [91,99,100], coupling with other non–noble elements into alloys or spinel structures [100,101], or composing bimetallics with noble metals [10,53,74–76,84]. Ruthenium is one of the most used noble metals for this purpose. The addition of Ru to an Ni catalyst enhances the Ni reducibility and dispersion on the catalyst surface [76,77] and increases the catalytic activity at a low temperature in CO_2 methanation [53,74]. In dry reforming of methane (DRM), the addition of Ru modifies the interaction between Ni and the support, improving catalyst stability and catalytic performance. The example could be Ru–Ni/Al_2O_3. However, in this way we can also reduce the performance by decreasing the interaction between Ni and the spinel as in Ru–Ni/$MgAl_2O_4$ [83]. In turn, it is suggested that Ru atoms probably block the most reactive Ni sites (step–edge sites) in an Ni–Ru/MgAl catalyst, leaving fewer reactive centers for methane activation (terraces), which favors carbon gasification and prevents CO dissociation [84]. Furthermore, the H_2:CO ratio in the RM is shifted to lower values for ruthenium–nickel catalysts in compared to catalysts that contain only nickel particles [98]. A Ru additive appeared also advantageous in the production of hydrogen via the steam reforming of simulated bio-oil (glycerol, syringol, n–butanol, m–xylene, m–cresol and furfural), where Ru affects the activity of the Ni/CeO_2–Al_2O_3 catalyst and significantly improves the H_2 yield, thereby increasing the reducibility of the Ni^{2+} species and minimizing the carbon deposition [10]. The addition of Ru into Ni catalysts often not only improves the overall conversion of a reactant but can also modify the product distribution. In the hydrogenolysis of lignin, for example, the introduction of Ru into an Ni/(activated carbon) catalyst increases the relative content of propyl guaiacol and propyl syringol in the products [11]. Ru also plays a role in photocatalysis. For example, in the metal–organic framework (Ru–UiO–67), photoelectrons are produced by Ru and delivered to the Ni(II) catalyst, which ultimately produces Ni^0 species for reducing CO_2 to CO [102]. In turn, Ru catalyst can be unblocked by photoexcitation of the adsorbed CO_2 [103]. Furthermore, Chen et al. described recently a photocatalyst consisting of monocrystalline metal selenide particles as a carrier and a bimetallic Ni-Ru system as a cocatalyst for very efficient hydrogen evolution reaction (HER) from the water [87]. They reported that the optimal catalyst composition contains 1.0 wt. Ni and 0.3 wt.%. Ru, and for such a material the apparent quantum yield (AQY) is 13.7% (highest H2 evolution rate of 2390 μmol h^{-1}) at 420 nm, which is the highest value recorded so far in the literature for HER photocatalysts with an absorption edge above 700 nm.

The properties of bimetallics are not a simple statistical result of the presence of these metals but results from the synergy, i.e., ensemble or ligand effect [38,95], which was discussed in Section 3 of this review. For the Ru–Ni catalysts, synergistic effects are highly probable because the metal particles are small and highly dispersed. This results in additional surface active sites [11]. Activity and selectivity is strongly dependent on the particle size [95]. In this context, Lange et al. constructed bimetallic RuNi catalysts that were supported on ZrO_2 in two series (low metal loading ca. 1 wt.% and higher metal loading in the range of 2–4 wt.%) with equal molar metal amounts in CO_2 methanation at 300–400 °C and 10 bar. The Ru–Ni bimetallic particles at the low loading on the support produced an optimum Ru:Ni ratio for 53:47 compared to the samples with a 0:1, 15:85, 31:69 or 1:0 ratio. Interestingly, for the higher metal loading, the bimetallic combinations turned out to be worse than the reference Ru or Ni monometallic material [78]. In bimetallic systems, an equally important factor for catalytic activity as well as for determining the course of the reaction path is the coordination of the atoms and the atomic structure of the metal surface [104]. For instance, the surfaces of Ni or Ru–Ni catalysts with low–coordinated atoms significantly reduce the global activation energy barrier for methane

or methanol formation from CO and H_2. In turn, the doped Ru-corrugated surface Ni (110) favors methane formation with respect to methanol formation. This is schematically shown in Figure 5 where the methane pathway is subject to less activation energy than the methanol pathway.

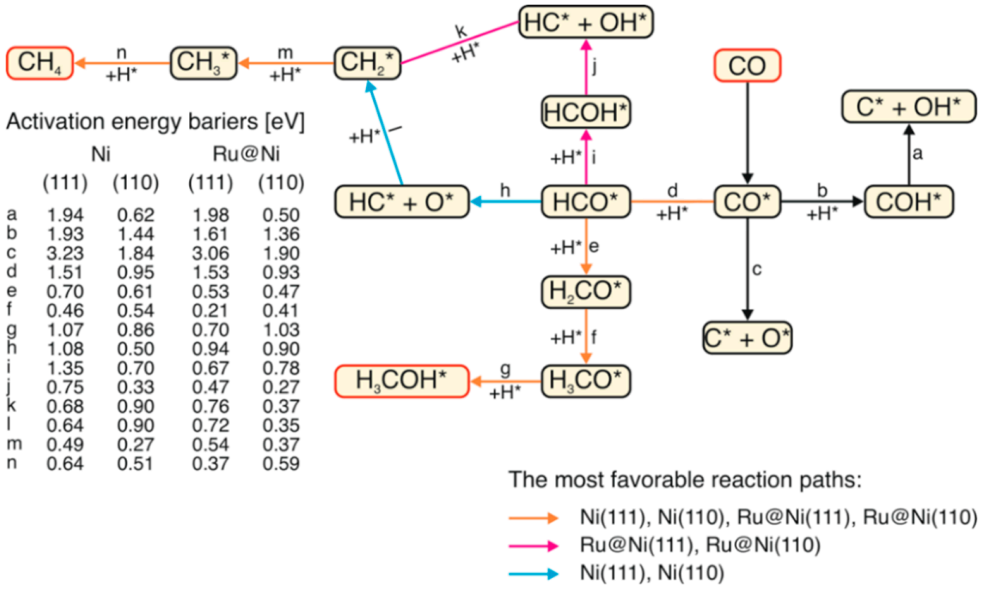

Figure 5. Scheme for the formation of methane and methanol from CO and H_2 on Ni (111), Ni (110), Ru@Ni (111) and Ru@Ni (110) surfaces, where asterisk indicates chemisorbed species. According to [104].

Low temperature is an important requirement for the catalysis of an exothermic CO_2 methanation reaction [99]. At temperatures higher than 320 °C, a competitive reaction, that is, a reverse water gas shift reaction (RWGS reaction), gets to be important [101,105]. This, in turn, leads to a formation of by-products such as CO, which is undesirable. Furthermore, at a low temperature, the sintering of the active species on the catalryst surface can be avoided [91,101]. A low temperature is also a clear advantage in the context of energy consumption [73]. In Table 3, we listed some of the examples of the Ru-Ni catalysts for low-temperature CO_2 or CO methanation.

Table 3. Ru-Ni catalysts for low-temperature methanation of CO or CO_2.

Catalysts (wt.%)	Reagent	WHSV ($L \cdot g^{-1} \cdot h^{-1}$)	T (°C)	Conv. (%)	TOF (h^{-1})	Ref.
0.5% Ru/Al_2O_3	CO_2	5.0	430	71	20.9	[106]
0.39% Ru/NiMgAl	CO_2	2.4	350	83	121.2	[79]
2.39% Ru/TiO2	CO_2	3.0	350	88	260.6	[107]
2.41% Ru/TiO2	CO_2	3.0	375	74	260.6	[107]
1.0% Ru/Ni nanowires	CO_2	15.0	179	100	24.8	[75]
1.5% Ru/Ni	CO_2	15.0	204	100	14.1	[53]
3% Ru-30% $Ni/Ce_{0,9}Zr_{0,1}O_2$	CO_2	2.4	230	98.2	no data	[74]
1% Ru–15% Ni/CeZr	CO_2	24.0	350	53	no data	[77]
0.5% Ru–20%Ni/Al_2O_3	CO_2	56.0	350	84.9	no data	[76]
9.2% Ni 0.8%Ru/SiO_2	CO	3.6	320	100	2.24	[80]
6.5% Ni@Ru–La_2O_3/SiO_2	CO	90.0	280	97	46.2	[81]
20% Ni 0.5% Ru/SiO_2	CO	40.0	275	80	21.4	[82]
1.44% Ru/Ni	CO	15.0	178	100	9.89	[73]
1.44% Ru/Ni	CO	15.0	−7	1.2	0.12	[73]

Ru/Ni conjugate appeared highly active at low temperature (entry 6 in Table 3) [53]. Interestingly, a special method for preparing a catalyst produces an unalloyed bimetallic construct [38,53,75,108].

We recently discovered a nano–Ru/nanowired–Ni system that is active starting from ca. 125 °C (onset of the reaction) and at 179 °C. In such conditions, 100% conversion and 100% selectivity to methane could be achieved for the TOF value of 2479.2 [75]. A bimetallic catalyst was constructed of the oxidized forms of the metals. On the surface of this catalyst, the Ni and Ru mainly occurred in the form of Ni $(OH)_2$ and RuO_2. Up to ca. 92% of Ni was in the form of Ni^{2+} and only 4% was in the form of Ni^0. The presence of the non-stoichiometric oxides RuO_x apparently plays a role in a high catalytic activity of Ru/Ni systems because generally catalyst's activity is often positively affected by non-stoichiometric compounds [6]. The high activity of a nano–Ru/nanowired–Ni system is additionally supported due to the high porosity of the Ni nanowires, which amounts to 99.31% and reaches a level of aerogels [75].

Catalyst support is an important issue for determining low-temperature performance [99,100]. The catalyst specified in Table 3 entry 7 is a good example. In $Ce_xZr_{1-x}O_2$ ($CeZrO_2$) supported Ni or Ru–Ni catalysts, it is the high oxygen storage capacity of the $CeZrO_2$ solid solution together with the presence of highly dispersed metal particles that yields a high efficiency [74,100,109]. In addition, the $Ce_xZr_{1-x}O_2$ support is characterized by a large amount of the basic active sites, which improves the chemisorption of the acidic CO_2 and prevents carbon deposition on the catalyst [110]. The preparation of the 3% Ru–30% Ni/$Ce_{0,9}Zr_{0,1}O_2$ catalyst is also worth noticing here. The catalyst was prepared using one-pot hydrolysis, which appeared to be better than the conventional impregnation method. Accordingly, the catalyst that was prepared using this procedure produced a higher activity at low temperatures and achieved a 98.2% CO_2 conversion with 100% selectivity to methane at 230 °C, where the catalyst was not deactivated after 300 h of operation [74].

The 1% Ru–15% Ni/CeZr and 0.5% Ru–20% Ni/Al_2O_3 catalysts (Table 3, entries 8 and 9) did not have an impressive efficiency. However, they did have some important advantages. The 1% Ru–15% Ni/CeZr system can be used in both CO_2 methanation and RWGS reactions [77]. It is extremely stable and maintained a CO_2 conversion of 53% at 350 °C in methanation (selectivity to CH4: 93%), while maintaining a CO_2 conversion of 72% at 700 °C in a RWGS reaction (selectivity to CO: 91%). In turn, the Ru–20% Ni/Al_2O_3 system (Table 3, entry 9) appeared to be very efficient in biogas upgrading via direct CO_2 methanation [76]. The initial concentration of CH_4 that was contained in biogas only slightly affected its catalytic efficiency. This technology seems to be strategic for eliminating the need to separate CO_2 from biogas, which usually takes place in the energy-intensive process of amine absorption [111]. Another important method in environmental technology is CO methanation used in syngas engineering, an important green chemistry concept. In Table 3, we listed several data for low temperature CO methanation under an Ru/Ni catalysis. We reported recently ultra-low temperature methanation of CO. Interestingly, the reaction can proceed in flow at as low temperatures as −7 °C under Ru/Ni catalysis but not under Re/Ni or Pd/Ni [73].

7. Mechanisms for Carbon (Di)oxide Hydrogenation

Although lexically bimetallic combination refers to metals, in practice, these structures are much more complex and can include various metal or metal oxide structures. An example of recent investigations is the research on the mechanism of the hydrogenation performance of Ru/Ni/C combinations. Ru–Ni–NiO or RuO_2–NiO interfaces were formed and both had a completely different mechanism. The Ru–Ni–NiO structures were reduced to metallic Ru (and to a lesser extent to metallic Ni), which then produced the so-called hydrogen spillover [85,112–119], and as a result, there is a synergic formation of Ru, Ni and NiO active sites. In turn, a similar synergy was not observed for the RuO_2–NiO structures [86].

Actually, metal oxides are active catalysts for carbon dioxide methanation. In Figure 6, we present a reaction mechanism that engages metal oxides and reacting CO_2 in forming carbonates or formats. A comprehensive review of the problem of the catalytic hydrogenation of CO_2 by metal oxides is available in the review [6].

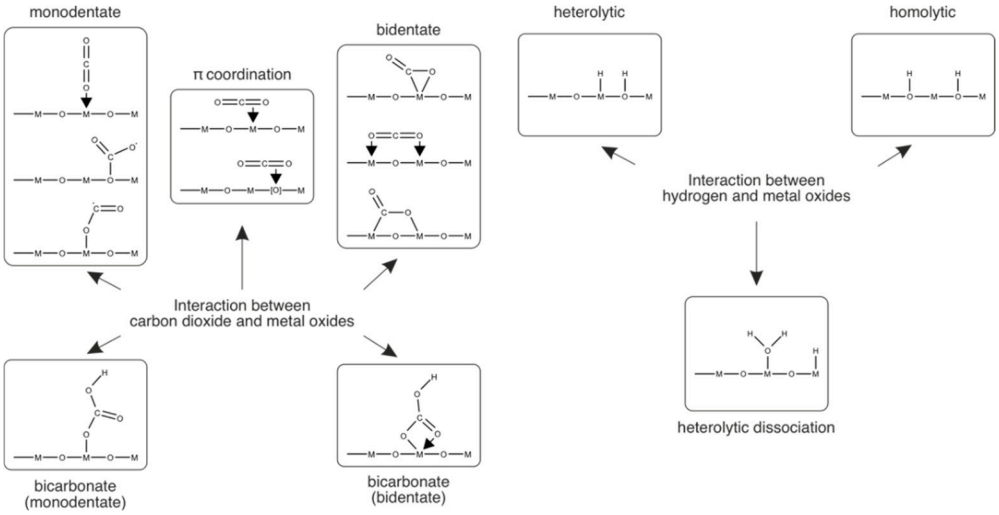

Figure 6. Different modes of the interactions of the CO_2 (**left**) and H_2 (**right**) reactants in methanation on stoichiometric and non-stoichiometric metal oxides. C—carbon, O—oxygen, [O]—oxygen vacancies, M—metal. According to [6].

8. Conclusions

Environmental catalysis is an important area of nanocatalysis. We reviewed here the different catalysts of this type, finding application, in particular, in carbon (di)oxide methanation. Synergy, ensemble and ligand effects are theoretical foundations explaining the advantages of multicomponent catalysis. Economic effect in multicomponent catalysis is an important issue for bimetallics. Low temperature (ultra-low temperature) and photocatalytic processes could be indicated as new tendencies in carbon (di)oxide methanation. In drug design, the exceptional popularity and success of some molecular fragments within the drug molecules population has a label of privileged structures. In analogy to this term, the efficiency and outstanding physico-chemical performance of the Ru/Ni combinations evoke a term privileged element for Ru and Ni in catalysis. In particular, Ru-based catalysts paved a bumpy road in a variety of commercial applications from ammonia synthesis to carbon (di)oxide methanation.

Author Contributions: Conceptualization, J.P., D.L.; formal analysis, J.P., M.K. and A.S.; writing—original draft preparation, J.P., D.L., M.K., P.B.; writing—review and editing, J.P., A.S., T.S., D.L., M.K.; visualization, D.L., T.S., P.B.; supervision, J.P. and A.S.; project administration, J.P. and D.L.; funding acquisition, J.P. All authors have read and agreed to the published version of the manuscript.

Funding: This research was funded by the National Science Center OPUS 2018/29/B/ST8/02303.

Conflicts of Interest: The authors declare no conflict of interest. The funders had no role in the design of the study; in the collection, analyses or interpretation of data; in the writing of the manuscript or in the decision to publish the results.

References

1. Smith, M.R.; Myers, S.S. Impact of anthropogenic CO_2 emissions on global human nutrition. *Nat. Clim. Chang.* **2018**, *8*, 834–839. [CrossRef]
2. Fletcher, S.E.M. Ocean circulation drove increase in CO_2 uptake. *Nature* **2017**, *542*, 169–170. [CrossRef] [PubMed]
3. DeVries, T.; Holzer, M.; Primeau, F. Recent increase in oceanic carbon uptake driven by weaker upper-ocean overturning. *Nature* **2017**, *542*, 215–218. [CrossRef] [PubMed]
4. Anastas, P.T.; Warner, J.C. *Green Chemistry: Theory and Practice*; Oxford University Press: Oxford, UK; New York, NY, USA, 1998; ISBN 978-0-19-850234-0.
5. Rodríguez-Padrón, D.; Puente-Santiago, A.R.; Balu, A.M.; Muñoz-Batista, M.J.; Luque, R. Environmental Catalysis: Present and Future. *ChemCatChem* **2019**, *11*, 18–38. [CrossRef]

6. Jia, J.; Qian, C.; Dong, Y.; Li, Y.F.; Wang, H.; Ghoussoub, M.; Butler, K.T.; Walsh, A.; Ozin, G.A. Heterogeneous catalytic hydrogenation of CO_2 by metal oxides: Defect engineering—Perfecting imperfection. *Chem. Soc. Rev.* **2017**, *46*, 4631–4644. [CrossRef]
7. Alshammari, A.; Kalevaru, V.; Martin, A. Bimetallic catalysts containing gold and palladium for environmentally important reactions. *Catalysts* **2016**, *6*, 97. [CrossRef]
8. Sinfelt, J.H. *Bimetallic Catalysts: Discoveries, Concepts, and Applications*; Wiley: New York, NY, USA, 1983; ISBN 978-0-471-88321-0.
9. Calzada Hernandez, A.R.; Gibran González Castañeda, D.; Sánchez Enriquez, A.; de Lasa, H.; Serrano Rosales, B. Ru-Promoted Ni/γAl_2O_3 fluidized catalyst for biomass gasification. *Catalysts* **2020**, *10*, 316. [CrossRef]
10. Italiano, C.; Bizkarra, K.; Barrio, V.L.; Cambra, J.F.; Pino, L.; Vita, A. Renewable hydrogen production via steam reforming of simulated bio-oil over Ni-based catalysts. *Int. J. Hydrogen Energy* **2019**, *44*, 14671–14682. [CrossRef]
11. Zhu, C.; Cao, J.-P.; Zhao, X.-Y.; Xie, T.; Zhao, M.; Wei, X.-Y. Bimetallic effects in the catalytic hydrogenolysis of lignin and its model compounds on Nickel-Ruthenium catalysts. *Fuel Process. Technol.* **2019**, *194*, 106126. [CrossRef]
12. Khan, Z. Trimetallic nanoparticles: Synthesis, characterization and catalytic degradation of formic acid for hydrogen generation. *Int. J. Hydrogen Energy* **2019**, *44*, 11503–11513. [CrossRef]
13. Polshettiwar, V.; Asefa, T. (Eds.) *Nanocatalysis: Synthesis and Applications*; John Wiley & Sons, Inc.: Hoboken, NJ, USA, 2013; ISBN 978-1-118-14886-0.
14. Musiol, R.; Mrozek-Wilczkiewicz, A.; Polanski, J. Synergy against fungal pathogens: Working together is better than working alone. *Curr. Med. Chem.* **2014**, *21*, 870–893. [CrossRef] [PubMed]
15. Gao, F.; Goodman, D.W. Pd–Au bimetallic catalysts: Understanding alloy effects from planar models and (supported) nanoparticles. *Chem. Soc. Rev.* **2012**, *41*, 8009. [CrossRef] [PubMed]
16. Spivey, J.J.; Agarwal, S.K. (Eds.) *Catalysis*; Royal Society of Chemistry: Cambridge, UK, 2007; Volume 11, ISBN 978-0-85186-654-3.
17. Shi, J. On the synergetic catalytic effect in heterogeneous nanocomposite catalysts. *Chem. Rev.* **2013**, *113*, 2139–2181. [CrossRef] [PubMed]
18. Morse, M.D. Clusters of transition-metal atoms. *Chem. Rev.* **1986**, *86*, 1049–1109. [CrossRef]
19. Allred, A.L. Electronegativity values from thermochemical data. *J. Inorg. Nucl. Chem.* **1961**, *17*, 215–221. [CrossRef]
20. Allen, L.C. Electronegativity is the average one-electron energy of the valence-shell electrons in ground-state free atoms. *J. Am. Chem. Soc.* **1989**, *111*, 9003–9014. [CrossRef]
21. Mann, J.B.; Meek, T.L.; Knight, E.T.; Capitani, J.F.; Allen, L.C. Configuration energies of the d-block elements. *J. Am. Chem. Soc.* **2000**, *122*, 5132–5137. [CrossRef]
22. Morss, L.R.; Edelstein, N.M.; Fuger, J.; Katz, J.J. (Eds.) *The Chemistry of the Actinide and Transactinide Elements*, 3rd ed.; Springer: Dordrecht, The Netherlands, 2006; ISBN 978-1-4020-3555-5.
23. Taylor, S.; Spain, E.M.; Morse, M.D. Spectroscopy and electronic structure of jet-cooled NiPd and PdPt. *J. Chem. Phys.* **1990**, *92*, 2710–2720. [CrossRef]
24. Simard, B.; Lebeault-Dorget, M.-A.; Marijnissen, A.; Ter Meulen, J.J. Photoionization spectroscopy of dichromium and dimolybdenum: Ionization potentials and bond energies. *J. Chem. Phys.* **1998**, *108*, 9668–9674. [CrossRef]
25. Taylor, S.; Lemire, G.W.; Hamrick, Y.M.; Fu, Z.; Morse, M.D. Resonant two-photon ionization spectroscopy of jet-cooled Pt_2. *J. Chem. Phys.* **1988**, *89*, 5517–5523. [CrossRef]
26. Fricke, B. Superheavy elements a prediction of their chemical and physical properties. In *Recent Impact of Physics on Inorganic Chemistry*; Springer: Berlin/Heidelberg, Germany, 1975; Volume 21, pp. 89–144. ISBN 978-3-540-07109-9.
27. Lide, D.R. (Ed.) *CRC Handbook of Chemistry and Physics: A Ready-Reference Book of Chemical and Physical Data*, 88th ed.; CRC: Boca Raton, FL, USA; London, UK, 2008; ISBN 978-0-8493-0488-0.
28. Freiser, B.S. *Organometallic Ion Chemistry*; Kluwer Academic: Dordrecht, The Netherlands; London, UK, 1996; ISBN 978-94-009-0111-7.
29. Loh, S.K.; Lian, L.; Hales, D.A.; Armentrout, P.B. Collision-induced dissociation of iron ion (Fe^{2+}). *J. Phys. Chem.* **1988**, *92*, 4009–4012. [CrossRef]

30. Pinegar, J.C.; Langenberg, J.D.; Arrington, C.A.; Spain, E.M.; Morse, M.D. Ni_2 revisited: Reassignment of the ground electronic state. *J. Chem. Phys.* **1995**, *102*, 666–674. [CrossRef]
31. Langenberg, J.D.; Morse, M.D. The bond energy of Rh2. *J. Chem. Phys.* **1998**, *108*, 2331–2335. [CrossRef]
32. Wang, H.; Liu, Y.; Haouari, H.; Craig, R.; Lombardi, J.R.; Lindsay, D.M. Raman spectra of ruthenium dimers. *J. Chem. Phys.* **1997**, *106*, 6534–6537. [CrossRef]
33. Liu, H. *Ammonia Synthesis Catalysts: Innovation and Practice*; World Scientific: Singapore, 2013; ISBN 978-981-4355-78-0.
34. Younas, M.; Loong Kong, L.; Bashir, M.J.K.; Nadeem, H.; Shehzad, A.; Sethupathi, S. Recent advancements, fundamental challenges, and opportunities in catalytic methanation of CO_2. *Energy Fuels* **2016**, *30*, 8815–8831. [CrossRef]
35. Cordero, B.; Gómez, V.; Platero-Prats, A.E.; Revés, M.; Echeverría, J.; Cremades, E.; Barragán, F.; Alvarez, S. Covalent radii revisited. *Dalton Trans.* **2008**, 2832. [CrossRef]
36. Tyson, W.R.; Miller, W.A. Surface free energies of solid metals: Estimation from liquid surface tension measurements. *Surf. Sci.* **1977**, *62*, 267–276. [CrossRef]
37. de Boer, F.R. (Ed.) *Cohesion in Metals: Transition Metal Alloys*; North Holland: Amsterdam, The Netherlands, 1988; ISBN 978-0-444-87098-8.
38. Zaleska-Medynska, A.; Marchelek, M.; Diak, M.; Grabowska, E. Noble metal-based bimetallic nanoparticles: The effect of the structure on the optical, catalytic and photocatalytic properties. *Adv. Colloid Interface Sci.* **2016**, *229*, 80–107. [CrossRef]
39. Fechete, I. Paul Sabatier—The father of the chemical theory of catalysis. *Comptes Rendus Chim.* **2016**, *19*, 1374–1381. [CrossRef]
40. Tieves, F.; Tonin, F.; Fernández-Fueyo, E.; Robbins, J.M.; Bommarius, B.; Bommarius, A.S.; Alcalde, M.; Hollmann, F. Energising the E-factor: The E+-factor. *Tetrahedron* **2019**, *75*, 1311–1314. [CrossRef]
41. Keijer, T.; Bakker, V.; Slootweg, J.C. Circular chemistry to enable a circular economy. *Nat. Chem.* **2019**, *11*, 190–195. [CrossRef] [PubMed]
42. Mond, L.; Langer, C.; Quincke, F.L. Action of carbon monoxide on nickel. *J. Chem. Soc. Trans.* **1890**, *57*, 749–753. [CrossRef]
43. Roduner, E. Understanding catalysis. *Chem. Soc. Rev.* **2014**, *43*, 8226–8239. [CrossRef] [PubMed]
44. Fischer, F.; Tropsch, H.; Dilthey, P. Reduction of carbon monoxide to methane in the presence of various metals. *Brennst. Chem.* **1925**, *6*, 265–271.
45. Graf, F.; Götz, M.; Henel, M.; Schaaf, T.; Tichler, R. *Technoökonomische Studie von Power-to-Gas-Konzepten*; DVGW: Bonn, Germany, 2014.
46. Ghaib, K.; Nitz, K.; Ben-Fares, F.-Z. Chemical methanation of CO_2: A review. *ChemBioEng Rev.* **2016**, *3*, 266–275. [CrossRef]
47. Jang, H.; Jin, W.; Nam, G.; Yoo, Y.; Jeon, J.S.; Park, J.; Kim, M.G.; Cho, J. Exploring the artificially induced nonstoichiometric effect of Li_2RuO_3 as a reactive promoter on electrocatalytic behavior. *Energy Environ. Sci.* **2020**, *13*, 2167–2177. [CrossRef]
48. Ananikov, V.P. Nickel: The "Spirited Horse" of Transition Metal Catalysis. *ACS Catal.* **2015**, *5*, 1964–1971. [CrossRef]
49. Sabatier, P. *Catalysis in Organic Chemistry*; Van Nostrand: New York, NY, USA, 1922.
50. Nørskov, J.K.; Bligaard, T.; Rossmeisl, J.; Christensen, C.H. Towards the computational design of solid catalysts. *Nat. Chem.* **2009**, *1*, 37–46. [CrossRef]
51. Andersson, M.; Bligaard, T.; Kustov, A.; Larsen, K.; Greeley, J.; Johannessen, T.; Christensen, C.; Norskov, J. Toward computational screening in heterogeneous catalysis: Pareto-optimal methanation catalysts. *J. Catal.* **2006**, *239*, 501–506. [CrossRef]
52. Lang, S.M.; Bernhardt, T.M.; Krstić, M.; Bonačić-Koutecký, V. The origin of the selectivity and activity of ruthenium-cluster catalysts for fuel-cell feed-gas purification: A gas-phase approach. *Angew. Chem. Int. Ed.* **2014**, *53*, 5467–5471. [CrossRef]
53. Polanski, J.; Siudyga, T.; Bartczak, P.; Kapkowski, M.; Ambrozkiewicz, W.; Nobis, A.; Sitko, R.; Klimontko, J.; Szade, J.; Lelątko, J. Oxide passivated Ni-supported Ru nanoparticles in silica: A new catalyst for low-temperature carbon dioxide methanation. *Appl. Catal. B Environ.* **2017**, *206*, 16–23. [CrossRef]
54. Gupta, S.S.; Singh, S.; Datta, J. Promoting role of unalloyed Sn in PtSn binary catalysts for ethanol electro-oxidation. *Mater. Chem. Phys.* **2009**, *116*, 223–228. [CrossRef]

55. Czerczak, S.; Gromiec, J.; Płaszewska-Tkacz, A.; Świdwińska-Gajewska, A.M. Nickel, ruthenium, rhodium, palladium, osmium, and platinum. In *Patty's Toxicology*; John Wiley & Sons, Inc.: Hoboken, NJ, USA, 2012; Volume 1.
56. Schutz, W. Ruthenium enhanced titanium alloys. *Platin. Met. Rev.* **1996**, *40*, 54–61.
57. Tin, S.; Yeh, A.C.; Ofori, A.P.; Reed, R.C.; Babu, S.S.; Miller, M.K. Atomic partitioning of ruthenium in ni-based superalloys. In Proceedings of the Superalloys 2004 (Tenth International Symposium), TMS, Champion, PA, USA, 19–23 September 2004; pp. 735–741.
58. Koizumi, Y.; Jianxin, Z.; Kobayashi, T.; Yokokawa, T.; Harada, H.; Aoki, Y.; Arai, M. Development of next generation ni-base single crystal superalloys containing ruthenium. *J. Jpn. Inst. Met.* **2003**, *67*, 468–471. [CrossRef]
59. Walston, S.; Cetel, A.; MacKay, R.; O'Hara, K.; Duhl, D.; Dreshfield, R. Joint development of a fourth generation single crystal superalloy. In Proceedings of the Superalloys 2004 (Tenth International Symposium), Champion, PA, USA, 19–23 September 2004; pp. 15–24.
60. Bondarenko, Y.A.; Kablov, E.N.; Surova, V.A.; Echin, A.B. Effect of high-gradient directed crystallization on the structure and properties of rhenium-bearing single-crystal alloy. *Met. Sci. Heat Treat.* **2006**, *48*, 360–363. [CrossRef]
61. Liu, N.; Yin, K.; Si, C.; Kou, T.; Zhang, Y.; Ma, W.; Zhang, Z. Hierarchically porous nickel–iridium–ruthenium–aluminum alloys with tunable compositions and electrocatalytic activities towards the oxygen/hydrogen evolution reaction in acid electrolyte. *J. Mater. Chem. A* **2020**, *8*, 6245–6255. [CrossRef]
62. Winter, M.; Brodd, R.J. What are batteries, fuel cells, and supercapacitors? *Chem. Rev.* **2004**, *104*, 4245–4270. [CrossRef]
63. Zhu, W.H.; Zhu, Y.; Davis, Z.; Tatarchuk, B.J. Energy efficiency and capacity retention of Ni–MH batteries for storage applications. *Appl. Energy* **2013**, *106*, 307–313. [CrossRef]
64. Willey, D.B.; Harris, I.R.; Pratt, A.S. The improvement of the hydrogenation properties of nickel-metal hydride battery alloy by surface modification with platinum group metals (PGMs). *J. Alloys Compd.* **1999**, *293–295*, 613–620. [CrossRef]
65. Willey, D.B.; Pederzolli, D.; Pratt, A.S.; Swift, J.; Walton, A.; Harris, I.R. Low temperature hydrogenation properties of platinum group metal treated, nickel metal hydride electrode alloy. *J. Alloy. Compd.* **2002**, *330–332*, 806–809. [CrossRef]
66. Chen, G.; Zou, N.; Chen, B.; Sambur, J.B.; Choudhary, E.; Chen, P. Bimetallic effect of single nanocatalysts visualized by super-resolution catalysis imaging. *ACS Cent. Sci.* **2017**, *3*, 1189–1197. [CrossRef]
67. An, K.; Somorjai, G.A. Nanocatalysis I: Synthesis of metal and bimetallic nanoparticles and porous oxides and their catalytic reaction studies. *Catal. Lett.* **2015**, *145*, 233–248. [CrossRef]
68. Roduner, E. *Nanoscopic Materials: Size-Dependent Phenomena and Growth Principles/ Emil Roduner*, 2nd ed.; Royal Society of Chemistry: Cambridge, UK, 2014; ISBN 978-1-84973-907-8.
69. Morag, A.; Maman, N.; Froumin, N.; Ezersky, V.; Rechav, K.; Jelinek, R. Nanostructured nickel/ruthenium/ruthenium-oxide supercapacitor displaying exceptional high frequency response. *Adv. Electron. Mater.* **2020**, *6*, 1900844. [CrossRef]
70. Zhou, G.; Xu, L.; Hu, G.; Mai, L.; Cui, Y. Nanowires for electrochemical energy storage. *Chem. Rev.* **2019**, *119*, 11042–11109. [CrossRef] [PubMed]
71. Trasatti, S.; Buzzanca, G. Ruthenium dioxide: A new interesting electrode material. Solid state structure and electrochemical behaviour. *J. Electroanal. Chem. Interfacial Electrochem.* **1971**, *29*, A1–A5. [CrossRef]
72. Sanchez-Sanchez, M.C.; Navarro Yerga, R.M.; Kondarides, D.I.; Verykios, X.E.; Fierro, J.L.G. Mechanistic aspects of the ethanol steam reforming reaction for hydrogen production on Pt, Ni, and PtNi catalysts supported on γ-Al_2O_3. *J. Phys. Chem. A* **2010**, *114*, 3873–3882. [CrossRef] [PubMed]
73. Siudyga, T.; Kapkowski, M.; Bartczak, P.; Zubko, M.; Szade, J.; Balin, K.; Antoniotti, S.; Polanski, J. Ultra-low temperature carbon (di)oxide hydrogenation catalyzed by hybrid ruthenium–nickel nanocatalysts: Towards sustainable methane production. *Green Chem.* **2020**. [CrossRef]
74. Shang, X.; Deng, D.; Wang, X.; Xuan, W.; Zou, X.; Ding, W.; Lu, X. Enhanced low-temperature activity for CO_2 methanation over Ru doped the Ni/CexZr(1−)O_2 catalysts prepared by one-pot hydrolysis method. *Int. J. Hydrogen Energy* **2018**, *43*, 7179–7189. [CrossRef]

75. Siudyga, T.; Kapkowski, M.; Janas, D.; Wasiak, T.; Sitko, R.; Zubko, M.; Szade, J.; Balin, K.; Klimontko, J.; Lach, D.; et al. Nano-Ru supported on Ni nanowires for low-temperature carbon dioxide methanation. *Catalysts* **2020**, *10*, 513. [CrossRef]
76. Stangeland, K.; Kalai, D.Y.; Li, H.; Yu, Z. Active and stable Ni based catalysts and processes for biogas upgrading: The effect of temperature and initial methane concentration on CO_2 methanation. *Appl. Energy* **2018**, *227*, 206–212. [CrossRef]
77. le Saché, E.; Pastor-Pérez, L.; Haycock, B.J.; Villora-Picó, J.J.; Sepúlveda-Escribano, A.; Reina, T.R. Switchable catalysts for chemical CO_2 recycling: A step forward in the methanation and reverse water–Gas shift reactions. *ACS Sustain. Chem. Eng.* **2020**, *8*, 4614–4622. [CrossRef]
78. Lange, F.; Armbruster, U.; Martin, A. Heterogeneously-catalyzed hydrogenation of carbon dioxide to methane using RuNi bimetallic catalysts. *Energy Technol.* **2015**, *3*, 55–62. [CrossRef]
79. Martins, J.A.; Faria, A.C.; Soria, M.A.; Miguel, C.V.; Rodrigues, A.E.; Madeira, L.M. CO_2 methanation over hydrotalcite-derived nickel/ruthenium and supported ruthenium catalysts. *Catalysts* **2019**, *9*, 1008. [CrossRef]
80. Yuan, C.; Yao, N.; Wang, X.; Wang, J.; Lv, D.; Li, X. The SiO_2 supported bimetallic Ni–Ru particles: A good sulfur-tolerant catalyst for methanation reaction. *Chem. Eng. J.* **2015**, *260*, 1–10. [CrossRef]
81. Li, S.; Gong, D.; Tang, H.; Ma, Z.; Liu, Z.-T.; Liu, Y. Preparation of bimetallic Ni@Ru nanoparticles supported on SiO_2 and their catalytic performance for CO methanation. *Chem. Eng. J.* **2018**, *334*, 2167–2178. [CrossRef]
82. Liu, Y.; Sheng, W.; Hou, Z.; Zhang, Y. Homogeneous and highly dispersed Ni–Ru on a silica support as an effective CO methanation catalyst. *RSC Adv.* **2018**, *8*, 2123–2131. [CrossRef]
83. Andraos, S.; Abbas-Ghaleb, R.; Chlala, D.; Vita, A.; Italiano, C.; Laganà, M.; Pino, L.; Nakhl, M.; Specchia, S. Production of hydrogen by methane dry reforming over ruthenium-nickel based catalysts deposited on Al_2O_3, $MgAl_2O_4$, and YSZ. *Int. J. Hydrogen Energy* **2019**, *44*, 25706–25716. [CrossRef]
84. Álvarez, A.M.; Bobadilla, L.F.; Garcilaso, V.; Centeno, M.A.; Odriozola, J.A. CO_2 reforming of methane over Ni-Ru supported catalysts: On the nature of active sites by operando DRIFTS study. *J. CO_2 Util.* **2018**, *24*, 509–515. [CrossRef]
85. Zhu, L.; Jiang, Y.; Zheng, J.; Zhang, N.; Yu, C.; Li, Y.; Pao, C.-W.; Chen, J.-L.; Jin, C.; Lee, J.-F.; et al. Ultrafine nanoparticle-supported ru nanoclusters with ultrahigh catalytic activity. *Small* **2015**, *11*, 4385–4393. [CrossRef]
86. Zhu, L.; Zhang, H.; Ma, N.; Yu, C.; Ding, N.; Chen, J.-L.; Pao, C.-W.; Lee, J.-F.; Xiao, Q.; Chen, H.B. Tuning the interfaces in the ruthenium-nickel/carbon nanocatalysts for enhancing catalytic hydrogenation performance. *J. Catal.* **2019**, *377*, 299–308. [CrossRef]
87. Chen, S.; Vequizo, J.J.M.; Hisatomi, T.; Nakabayashi, M.; Lin, L.; Wang, Z.; Yamakata, A.; Shibata, N.; Takata, T.; Yamada, T.; et al. Efficient photocatalytic hydrogen evolution on single-crystalline metal selenide particles with suitable cocatalysts. *Chem. Sci.* **2020**, *11*, 6436–6441. [CrossRef]
88. Stangeland, K.; Kalai, D.; Li, H.; Yu, Z. CO_2 methanation: The effect of catalysts and reaction conditions. *Energy Procedia* **2017**, *105*, 2022–2027. [CrossRef]
89. Gao, J.; Liu, Q.; Gu, F.; Liu, B.; Zhong, Z.; Su, F. Recent advances in methanation catalysts for the production of synthetic natural gas. *RSC Adv.* **2015**, *5*, 22759–22776. [CrossRef]
90. Olah, G.A.; Goeppert, A.; Prakash, G.K.S. *Beyond Oil and Gas: The Methanol Economy*; Wiley-VCH: Weinheim, Germany, 2011; ISBN 978-3-527-64463-6.
91. Rönsch, S.; Schneider, J.; Matthischke, S.; Schlüter, M.; Götz, M.; Lefebvre, J.; Prabhakaran, P.; Bajohr, S. Review on methanation—From fundamentals to current projects. *Fuel* **2016**, *166*, 276–296. [CrossRef]
92. Agrafiotis, C.; Roeb, M.; Sattler, C. A review on solar thermal syngas production via redox pair-based water/carbon dioxide splitting thermochemical cycles. *Renew. Sustain. Energy Rev.* **2015**, *42*, 254–285. [CrossRef]
93. Gao, J.; Wang, Y.; Ping, Y.; Hu, D.; Xu, G.; Gu, F.; Su, F. A thermodynamic analysis of methanation reactions of carbon oxides for the production of synthetic natural gas. *RSC Adv.* **2012**, *2*, 2358. [CrossRef]
94. Mizuno, N.; Misono, M. Heterogeneous catalysis. *Chem. Rev.* **1998**, *98*, 199–218. [CrossRef]
95. Liu, L.; Corma, A. Metal catalysts for heterogeneous catalysis: From single atoms to nanoclusters and nanoparticles. *Chem. Rev.* **2018**, *118*, 4981–5079. [CrossRef]
96. Shiju, N.R.; Guliants, V.V. Recent developments in catalysis using nanostructured materials. *Appl. Catal. Gen.* **2009**, *356*, 1–17. [CrossRef]
97. Argyle, M.; Bartholomew, C. Heterogeneous catalyst deactivation and regeneration: A review. *Catalysts* **2015**, *5*, 145–269. [CrossRef]

98. Wysocka, I.; Hupka, J.; Rogala, A. Catalytic activity of nickel and ruthenium–nickel catalysts supported on SiO_2, ZrO_2, Al_2O_3, and $MgAl_2O_4$ in a dry reforming process. *Catalysts* **2019**, *9*, 540. [CrossRef]
99. Lee, W.J.; Li, C.; Prajitno, H.; Yoo, J.; Patel, J.; Yang, Y.; Lim, S. Recent trend in thermal catalytic low temperature CO_2 methanation: A critical review. *Catal. Today* **2020**. [CrossRef]
100. Qin, Z.; Zhou, Y.; Jiang, Y.; Liu, Z.; Ji, H. Recent advances in heterogeneous catalytic hydrogenation of CO_2 to methane. In *New Advances in Hydrogenation Processes—Fundamentals and Applications*; Ravanchi, M.T., Ed.; InTech: London, UK, 2017; ISBN 978-953-51-2869-4.
101. Mills, G.A.; Steffgen, F.W. Catalytic methanation. *Catal. Rev.* **1974**, *8*, 159–210. [CrossRef]
102. Yan, Z.-H.; Ma, B.; Li, S.-R.; Liu, J.; Chen, R.; Du, M.-H.; Jin, S.; Zhuang, G.-L.; Long, L.-S.; Kong, X.-J.; et al. Encapsulating a Ni (II) molecular catalyst in photoactive metal–organic framework for highly efficient photoreduction of CO_2. *Sci. Bull.* **2019**, *64*, 976–985. [CrossRef]
103. Kim, C.; Hyeon, S.; Lee, J.; Kim, W.D.; Lee, D.C.; Kim, J.; Lee, H. Energy-efficient CO_2 hydrogenation with fast response using photoexcitation of CO_2 adsorbed on metal catalysts. *Nat. Commun.* **2018**, *9*, 3027. [CrossRef]
104. Fajín, J.L.C.; Gomes, J.R.B.; Natália, M.; Cordeiro, M.N. Mechanistic study of carbon monoxide methanation over pure and rhodium- or ruthenium-doped nickel catalysts. *J. Phys. Chem. C* **2015**, *119*, 16537–16551. [CrossRef]
105. Xiaoding, X.; Moulijn, J.A. Mitigation of CO_2 by chemical conversion: Plausible chemical reactions and promising products. *Energy Fuels* **1996**, *10*, 305–325. [CrossRef]
106. Porta, A.; Falbo, L.; Visconti, C.G.; Lietti, L.; Bassano, C.; Deiana, P. Synthesis of Ru-based catalysts for CO_2 methanation and experimental assessment of intraporous transport limitations. *Catal. Today* **2020**, *343*, 38–47. [CrossRef]
107. Chai, S.; Men, Y.; Wang, J.; Liu, S.; Song, Q.; An, W.; Kolb, G. Boosting CO_2 methanation activity on Ru/TiO_2 catalysts by exposing (001) facets of anatase TiO_2. *J. CO_2 Util.* **2019**, *33*, 242–252. [CrossRef]
108. Serp, P.; Philippot, K. (Eds.) *Nanomaterials in Catalysis*; Wiley-VCH: Weinheim, Germany, 2013; ISBN 978-3-527-33124-6.
109. Ocampo, F.; Louis, B.; Roger, A.-C. Methanation of carbon dioxide over nickel-based Ce0.72Zr0.28O2 mixed oxide catalysts prepared by sol–gel method. *Appl. Catal. Gen.* **2009**, *369*, 90–96. [CrossRef]
110. Aziz, M.A.A.; Jalil, A.A.; Wongsakulphasatch, S.; Vo, D.-V.N. Understanding the role of surface basic sites of catalysts in CO_2 activation in dry reforming of methane: A short review. *Catal. Sci. Technol.* **2020**, *10*, 35–45. [CrossRef]
111. Chaemchuen, S.; Kabir, N.A.; Zhou, K.; Verpoort, F. Metal–organic frameworks for upgrading biogas via CO2 adsorption to biogas green energy. *Chem. Soc. Rev.* **2013**, *42*, 9304. [CrossRef] [PubMed]
112. Conner, W.C.; Falconer, J.L. Spillover in heterogeneous catalysis. *Chem. Rev.* **1995**, *95*, 759–788. [CrossRef]
113. Prins, R. Hydrogen spillover. Facts and fiction. *Chem. Rev.* **2012**, *112*, 2714–2738. [CrossRef]
114. Karim, W.; Spreafico, C.; Kleibert, A.; Gobrecht, J.; VandeVondele, J.; Ekinci, Y.; van Bokhoven, J.A. Catalyst support effects on hydrogen spillover. *Nature* **2017**, *541*, 68–71. [CrossRef]
115. Chen, H.; Yang, H.; Omotoso, O.; Ding, L.; Briker, Y.; Zheng, Y.; Ring, Z. Contribution of hydrogen spillover to the hydrogenation of naphthalene over diluted Pt/RHO catalysts. *Appl. Catal. Gen.* **2009**, *358*, 103–109. [CrossRef]
116. Xia, S.; Nie, R.; Lu, X.; Wang, L.; Chen, P.; Hou, Z. Hydrogenolysis of glycerol over Cu0.4/Zn5.6−xMgxAl2O8.6 catalysts: The role of basicity and hydrogen spillover. *J. Catal.* **2012**, *296*, 1–11. [CrossRef]
117. Chen, C.-Y.; Chang, J.-K.; Tsai, W.-T.; Hung, C.-H. Uniform dispersion of Pd nanoparticles on carbon nanostructures using a supercritical fluid deposition technique and their catalytic performance towards hydrogen spillover. *J. Mater. Chem.* **2011**, *21*, 19063. [CrossRef]
118. Jiang, N.; Rao, K.S.R.; Jin, M.-J.; Park, S.-E. Effect of hydrogen spillover in decalin dehydrogenation over supported Pt catalysts. *Appl. Catal. Gen.* **2012**, *425–426*, 62–67. [CrossRef]
119. Navarrete, C.; García, R.; Sepulveda, C.; Gil-Llambias, F.J.; Fierro, J.L.G.; Escalona, N. Deep hydrodesulphurization via hydrogen spillover. *Catal. Lett.* **2011**, *141*, 1796–1802. [CrossRef]